OPTIMIZATION OF CULTIVATION PARAMETERS FOR CO_2 SEQUESTRATION AND PROTEIN PRODUCTION IN *CHLORELLA VULGARIS* USING TAGUCHI METHODOLOGY

SOUMAYAT ALI IBRAHIM MZE [1], AZLIN SUHAIDA AZMI[1*], NOOR ILLI MOHAMAD PUAD [1], FARAH AHMAD[1], HASRIZAL B A RAHMAN[2], NURUL FARAHIN ABD WAHAB [2]

[1]*Dept. Chemical Engineering and Sustainability, Kulliyyah of Engineering, International Islamic University. Malaysia (IIUM), Jalan Gombak, 53100 Kuala Lumpur, Malaysia.*

[2] *PETRONAS Research Sdn Bhd. Lot 3288 & 3299, off Jalan Ayar Itam, Kawasan Institusi Bangi, 43000 Kajang, Selangor Darul Ehsan, Malaysia*

*Corresponding author: *azlinsu76@iium.edu.my*

ABSTRACT: Microalgae, known for their high photosynthetic efficiency, offer a promising approach for CO_2 sequestration and the production of high-value products such as single-cell proteins (SCP). However, low CO_2 solubility in water and strain-specific tolerance limit CO_2 fixation efficiency. This study aimed to optimize CO_2 fixation and SCP production in freshwater *Chlorella vulgaris* using the Taguchi Orthogonal Array method. Key parameters, namely light (5-15 kLx), CO_2 concentration (1–5%), and nitrogen content (0–1 g/L), were investigated in a 2-L Schott glass bottle. Process validation was performed within the same system, and a comparative assessment was subsequently conducted against a 2-L flat-panel photobioreactor (FPPBR) to determine any differences in cultivation performance. Results showed that biomass productivity had a greater influence on CO_2 fixation (9.05%) and protein yield (45.78%) than CO_2 concentration or nitrogen content. Notably, the flat-panel PBR achieved superior growth performance (47.67%), highlighting the importance of reactor design. Logistic growth modeling fitted with Taguchi-derived growth rates showed a good fit to the data ($R^2 = 0.6$–0.93), supporting the optimization framework. These findings provide valuable insights for enhancing microalgae CO_2 capture and SCP production, although further refinement of cultivation systems and kinetic models is necessary.

KEY WORDS: *carbon capture, carbon fixation, microalgae cultivation, single-cell protein.*

1. INTRODUCTION

Climate change driven by anthropogenic greenhouse gas emissions, particularly carbon dioxide (CO_2), poses a growing threat to global ecosystems and food security. With global CO_2 emissions reaching over 36 billion tons in 2022 alone, urgent and scalable mitigation strategies are needed to reduce atmospheric carbon levels and transition toward more sustainable resource systems [1].

Among proposed solutions, biological CO_2 fixation using microalgae has emerged as a promising approach due to its ability to capture carbon while simultaneously generating

high value bioproduct [2]. Through photosynthesis, microalgae convert CO_2 into oxygen and organic matter, with reported sequestration rates up to 513 tonnes of CO_2 per hectare per year—significantly outperforming terrestrial crops in fixation efficiency and growth rates [3].

Within this group, *Chlorella vulgaris* is particularly well-studied for carbon capture applications, thanks to its high tolerance to elevated CO_2 concentrations (up to 40%), robust growth in varied environments, and ability to accumulate large amounts of protein-rich biomass. These traits make *C. vulgaris* a suitable candidate for integration into circular bioeconomy models that require both waste carbon utilization and protein production [4].

Beyond CO_2 capture, *C. vulgaris* also serves as a sustainable source of single-cell protein (SCP), a protein-dense biomass derived from microbial or algal sources. SCP production offers a resource-efficient alternative to conventional protein systems like soy or fishmeal, with *C. vulgaris* typically containing 40–70% protein by dry weight, along with essential amino acids, lipids, and micronutrients [2,5]. Its potential to address global protein demands with minimal land and water use has drawn significant interest for use in food, feed, and nutraceutical applications.

However, the efficiency of CO_2 fixation and protein accumulation in *C. vulgaris* is highly sensitive to environmental and operational parameters, including light intensity, photoperiod, CO_2 concentration, and nitrogen availability [6]. These factors influence cellular metabolism, photosynthetic efficiency, and biochemical composition [6]. For instance, while optimal light drives photosynthesis, excessive intensity leads to photoinhibition [7]. Nitrogen availability governs protein biosynthesis, and CO_2 levels influence carbon assimilation and intracellular pH regulation [8–10]. These interactions are illustrated in Fig. 1 and Fig. 2, which summarizes the complex interplay between light, carbon, and nitrogen inputs that ultimately determine productivity in microalgal systems.

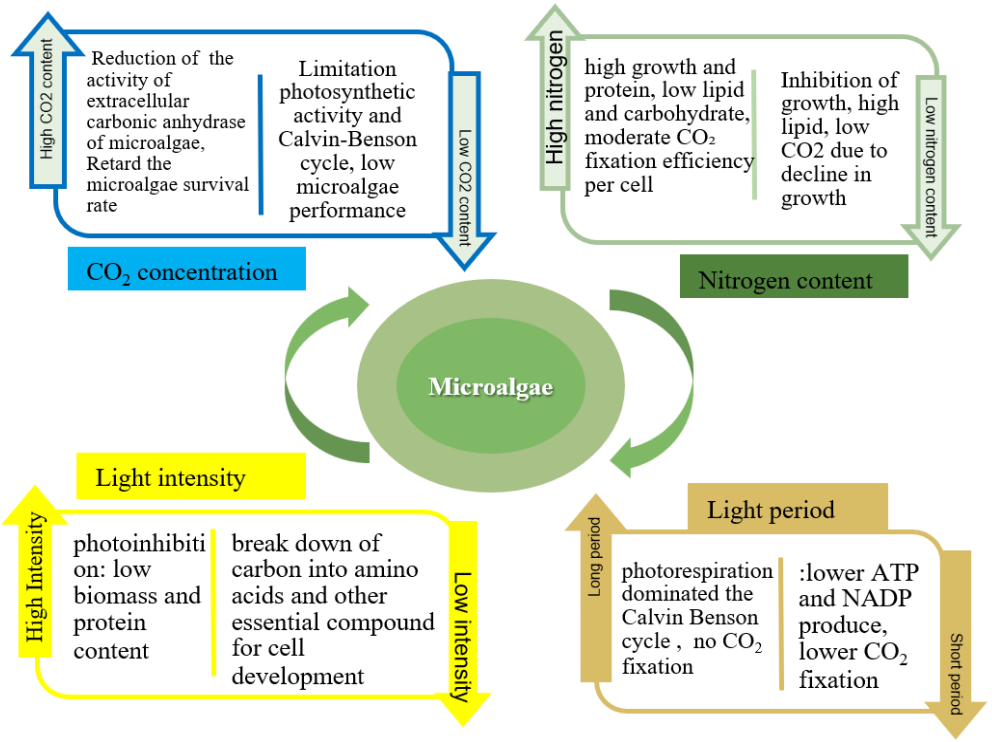

Fig. 1. Schematic representation of interacting cultivation parameters influencing *C. vulgaris* performance.

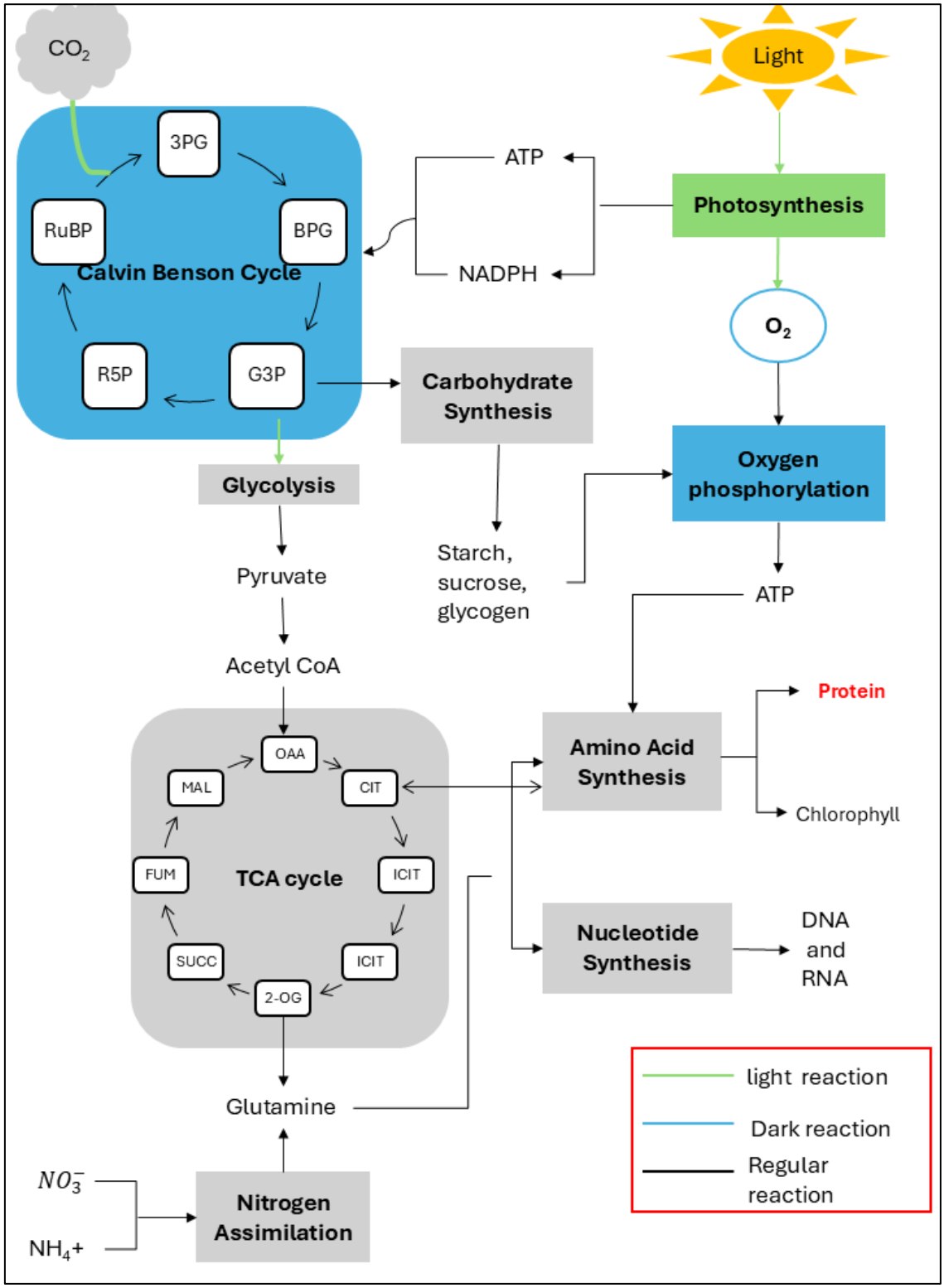

Fig. 2. Schematic overview of microalgae metabolism, illustrating major pathways such as the Calvin–Benson cycle, TCA cycle, glycolysis, and the synthesis of lipids and proteins.

To navigate this complexity, statistical design of experiments (DoE) is essential. The Taguchi Orthogonal Array (OA) method offers an efficient, low-cost approach to identifying significant process parameters with fewer experimental runs than traditional factorial designs [11]. This method has been successfully applied in algal systems to optimize lipid, pigment, and nutrient removal performance, but has rarely been used for dual-target optimization of CO_2 fixation and protein productivity in *C. vulgaris* [12–14].

Following process optimization, validation at scale becomes critical. While glass bottle photobioreactors (PBRs) are ideal for controlled laboratory studies, their hydrodynamics and light profiles differ substantially from flat-panel PBRs, which offer superior light distribution and CO_2 transfer efficiency [15,16]. As shown in prior studies through the review of Abdur Razzak [17], scaling up from bottle cultures to flat-panel systems often leads to performance changes due to reactor geometry. Thus, comparing growth and protein productivity in both systems is essential to assess the scalability and robustness of optimized conditions.

In parallel, kinetic growth modeling is crucial for understanding dynamic culture responses under varying environmental conditions [11]. It allows estimation of specific growth rates, biomass productivity, and CO_2 utilization efficiency—enabling process prediction and scale-up. Among the various models discussed previously [18–21], three studies were chosen to perform the kinetic growth fitting and to validate the system's growth performance to inform future scale-up strategies. The method selection criteria were based on the simplicity of the concept and the availability of all constants required for the research [18,22–24].

This study aims to fill these gaps by integrating Taguchi optimization and kinetic modeling to enhance CO_2 sequestration and SCP production in *C.vulgaris*. Optimized conditions are validated in both Schott bottles and flat-panel PBR systems, with comparative evaluation of productivity and growth dynamics to inform scalable bioprocess development.

2. METHODOLOGY

2.1. Microalgae and Culture Conditions

C.vulgaris provided by the Herbarium laboratory, IIUM, was the microalgae used in this study. 3N bold basal media (BBM) from Hasinah et al. (2023)[41] was used as the culture medium for this project, with slight modifications to the trace metal solutions used.

The inoculum culture was grown in a 500 mL Erlenmeyer flask with a working volume of 200 mL at a temperature of 27±2 °C under a fluorescent lamp (2.8 kLx: 33.73 µmol photons m^{-2} s^{-1}) with an illumination: dark period of 16:8 hr for 7 days before being transferred to a 2-L photobioreactor. The population density at the start of the experiment was set at 20% of the inoculum adjusted with media to 1 L of working volume (Taguchi analysis) and to 2 L for the flat panel PBR (comparison study).

2.2.1. Photobioreactor Setup

Two different photobioreactors were used in this study, which were a 2-L Schott bottle and a 2-L flat panel PBR. The first one was used for the Taguchi analysis, and the other one was used for the comparative study.

2.2.2. Schott Bottle Photobioreactors.

The Schott bottle photobioreactors used in this study is a 2-L Schott bottle (a working volume of 1 L) with a cover cap containing 3 holes; one hole to insert the gas tube for the sparging, one hole for the 30 mL sampling pot, and another one for the release of the exhaust gas connected to the CO_2 gas sensor (Fig. 3) to monitor the amount of CO_2 released from the system. The gas supply was provided using a stone sparger at 0.8 vvm. For the light source, three LED strips with adjustable light intensity were attached to black paper and positioned around the Schott bottle at a distance of 5 cm to prevent the bottle from heating during illumination (Fig. 3). To maintain the volume of the cultivation constant, 30 mL media was added daily to the culture after each sampling.

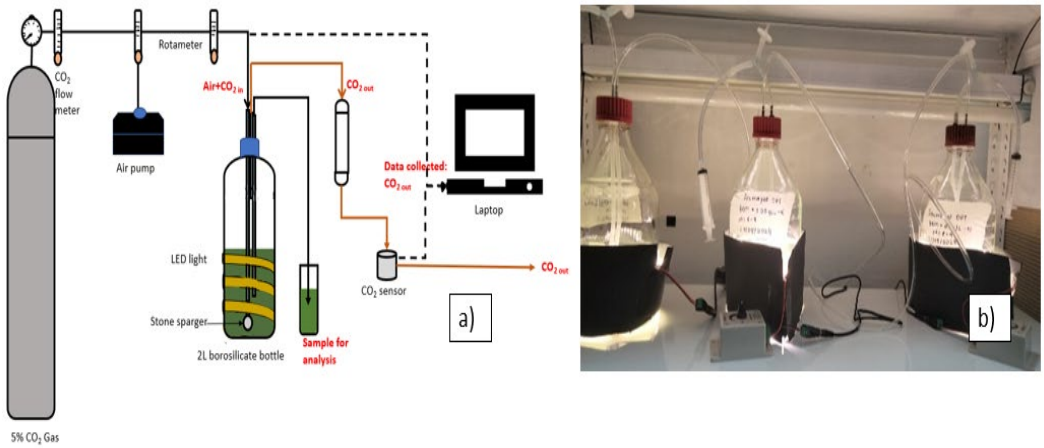

Fig. 3. Experimental Setup: (a) Schematic Diagram and (b) Actual Setup

2.2.3. Flat Panel Photobioreactor.

A glass flat panel photobioreactor with a 2 L working volume (359mm x 247 mm x 30 mm) was used for comparative purposes. The aeration was supplied at the bottom of the reactor using a metal rod at a rate of 0.8 vvm. The illumination was done using LED panel placed in one side of the PBR with adjustable light intensity. The sample was collected using a 30 mL syringe at the top of the PBR (Fig. 4).

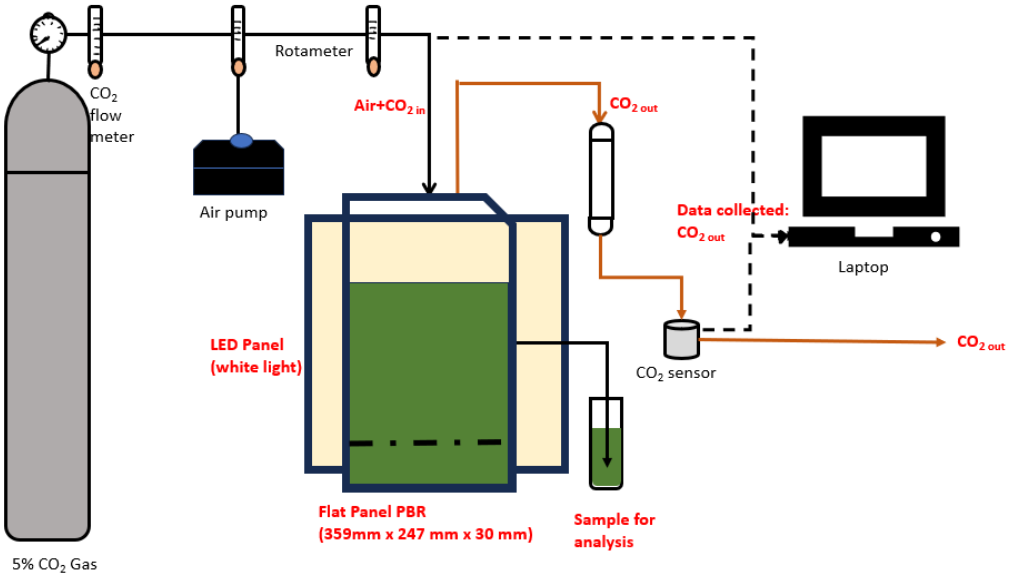

Fig. 4. Set up of the 2-L Flat panel PBR

2.3. Design of the Analysis of Process Parameters for Maximum CO_2 Fixation and SCP Production

An L9 (3^4) Taguchi Orthogonal Array (OA) design was employed using Design Expert v13 to optimize the cultivation parameters influencing the growth of *C. vulgaris*. Four independent variables were considered: CO_2 concentration (1, 3, and 5%), light intensity (5, 10, and 15 kLx), light period (8, 12, and 16 h), and nitrogen concentration (0, 0.05, and 0.1 g/L-N). The L9 array enabled systematic evaluation of these parameters at three levels each while reducing the number of experimental trials without compromising statistical accuracy. The experimental design matrix is presented in Table 1. The collected data were analyzed using a half-normal plot and analysis of variance (ANOVA) to determine the most influential factors and validate the optimized conditions.

Table 1: Summary of the Taguchi OA analysis

Factor	Name	Units	Low	Middle	High
1	CO_2 concentration	%	1	3	5
2	Light intensity	kLx	5	10	15
3	Light period	hr	8	12	16
4	Nitrogen concentration	g/L	0.00	0.05	0.10
Responses	Growth rate	day^{-1}			
	Protein productivity	g/L/day			
	CO_2 capture efficiency	%			

2.4. Analysis

2.4.1. Growth Evaluation.

The growth evaluation of microalgae cultivation was done based on Ayatullahi et al. (2021) and Paladino & Neviani (2024) [15,42], with slight modifications. The cell dry

weight (CDW) was determined through the gravimetric method, and the value was calculated using Eq. (1). Biomass productivity (Eq. (2)) and specific growth rate (Eq. (3)) were calculated based on the CDW value.

$$X_{biomass}(\frac{\mathrm{g}}{\mathrm{L}}) = \left(\frac{Final\ weigh\ of\ filter - Final\ weigh\ of\ filter}{Volume\ of\ sample}\right) \quad (1)$$

$$P_{biomass}\left(\frac{\frac{g}{l}}{day}\right) = \frac{X_2 - X_1}{t_2 - t_1} \quad (2)$$

$X_1$and X_2 were the biomass concentration measured respectively at the beginning t_1 and the end of the cultivation t_2.

$$\mu = \left(\frac{\ln\left(\frac{X_f}{X_i}\right)}{(t_f - t_i)}\right) \quad (3)$$

X_f and X_i were measured respectively at the end t_f and the beginning of the exponential phase t_i.

2.4.2. Carbon Concentration Analysis

To evaluate the overall carbon sequestration performance of the microalgae, CO_2 capture (Eq. (4), CO_2 bio fixation rate (Eq. (5), and CO_2 fixation efficiency (Eq. (6)) were also assessed based on the method obtained from Aghalipour et al. (2020) [39].

$$\mathrm{CO_2\ capture\ (\%)} = \frac{\mathrm{Average\ inlet\ concentration - Average\ outlet\ concentration}}{\mathrm{Average\ inlet\ concentration}}\ \mathrm{x}\ 100 \quad (4)$$

$$(\mathrm{R_{CO2}})\left(\frac{\frac{\mathrm{g}}{\mathrm{L}}}{\mathrm{day}}\right) = C_c\ \mathrm{x}\ \mathrm{P_{biomass}}\ \mathrm{x}\left(\frac{M_{CO2}}{M_C}\right) \quad (5)$$

$$E_{CO2}(\%) = \left(\frac{(R_{CO2} \times V)\left(\frac{g}{day}\right)}{F_{CO2}\left(\frac{g}{day}\right)}\right) \times 100 \quad (6)$$

Where R_{CO2} and E_{CO2} are the CO_2 fixation rate (g/L/day) and CO_2 fixation efficiency (%), respectively. C_c is the carbon content of the microalgae biomass (in %w/w) determined using the elemental analyzer, $P_{biomass}$ is the average biomass productivity, and M_{CO2} and M_C are the respective CO_2 and carbon molecular weights (g/mol). V is the working volume (L) and F_{CO2} is the CO_2 gas flow rate inlet (g/day).

2.4.3. Total Protein Content

The nitrogen contained in the bioreactor and the total protein content were determined by the elemental analyzer (CHNS analyzer). The nitrogen fixation rate and total protein content were calculated using Eqs (7) and (8), respectively.

$$\text{Nitrogen fixation rate (\%)} = \left(\frac{\left[X_{biomass} \times N_{algae}\right]}{TN}\right) \times 100\% \quad (7)$$

Where *TN* (mg/L) is the total nitrogen added to the culture medium (nitrate-N or ammonium-N). $X_{biomass}$ (mg/L) is the biomass concentration. N_{algae} is the nitrogen content of biomass.

$$Protein\ content\ (g/g) = N_{algae} \times 6.25 \quad (8)$$

Protein content was measured throughout the 14-day cultivation period to monitor its variation over time. Specific protein productivity (g/g/day) was calculated at each time point by dividing the protein content by the corresponding cultivation time. This method allowed for the assessment of protein synthesis rates during different growth phases of *C. vulgaris*.

$$Spefic\ \ protein\ productivity\left(\frac{g/g}{day}\right) = \left[protein\ content\ \left(\frac{g}{g}\right)\right]/times(day) \quad (9)$$

2.4.4. Lipid Content

Lipid determination was done using harvested microalgae that had been freeze-dried and stored at -20 °C freezer using the modified Bligh and Dyer method [43]. The equation used is as follows:

$$\text{Lipid content (\%)} = \frac{Weight\ of\ oil\ in\ aliquot\ (g)}{Weight\ of\ dried\ biomass\ (g)} \text{ x } 100 \quad (10)$$

2.5. Determination of Kinetic Growth

Three runs obtained from the optimized solution of the Taguchi analysis were chosen to determine the kinetic model. The biomass concentration and microalgae growth were determined using Equations (1) and (3), and the data were then fitted nonlinearly using a nonlinear regression feature in the Origin 2025 app. Four growth models were used to fit the data based on a good fit of $R^2 > 0.75$. These included the basic Logistic model (Eq. (11)) [22], modified Logistic (Eq. (12)), and Gompertz models (Eq. (13)) from Meng & Kassim (2020) [24], and a multi-factor model (Eq. (14)) adapted from Romagnoli et al. (2021) [18]. The latter was modified for this study by excluding temperature and phosphate, focusing instead on CO_2 concentration, nitrogen content, and light intensity (Eq. (14)).

$$Basic\ Logistic\ Model: X(t) = \frac{X_{max}}{1 + \left(\frac{X_{max}}{X_o} + 1\right) \times e^{-\mu_{max} \times t}} \quad (11)$$

$$Modified\ Logistic\ Model: X(t) = \frac{X_0 \times e^{Kt}}{1 - \left(\frac{X_0}{X_m}\right) \times (1 - e^{Kt})} \quad (12)$$

$$Gompertz\ model: X(t) = X_o \times \exp\left(-e^{K \times e^{\frac{1}{X_o}}}\right) \times (X_m - t) + 1 \quad (13)$$

$$\mu = \mu_{max} \times \left[\frac{S_N}{k_{(s,N)} + S_N} \times \frac{S_C}{k_{(s,C)} + S_C} \times \frac{I}{I_o} \times e^{\left(1 - \frac{I}{I_o}\right)}\right] \quad (14)$$

Where X_0 and X_m are the initial and maximum biomass concentration (g/L) respectively; *K* is the specific growth rate (day^{-1}) obtained from the Taguchi OA solution, and t is the cultivation time (day). The μ_{max} is the maximum specific growth rate (day $^{-1}$), S_N, and S_C are the concentrations of nitrogen and CO_2 inside the culture media, respectively (g/L). I_o is the average initial light intensity, I_s is the average saturated light intensity (µmol/ (m^2.s), while

$k_{(s,\ N)}$ and $k_{(s,\ C)}$ are constants retrieved from [18] research, in which each having a value of 0.0023 and 0.0046, respectively.

3. RESULTS AND DISCUSSION

3.1. Influence of Different Variables on Different Responses

The Taguchi OA design was applied to assess which parameters most significantly affect microalgal growth, CO_2 capture, and protein production, with the goal to optimize CO_2 uptake without compromising the other two responses. Table 2 shows that the highest growth rate (0.469 day^{-1}) occurred in Run 8 (3% CO_2,10 kLx, 8 hr,0.1 N-g/L), the maximum CO_2 capture (93.19%) in Run 7 (5% CO_2,15 kLx, 12 hr, 0.0 g/L-N), and the highest protein productivity (0.057 g/g/day) in Run 1 ((3% CO_2,15 kLx, 8 hr,0.05 g/L-N). These findings suggest that microalgae have strong potential in all three areas; however, the optimal conditions for each response differ, indicating they are not directly correlated [6]. Thus, to determine the most influential factors for each response, half-normal plots and ANOVA were used to distinguish significant factors from random variation, while the equations and the one-factor analysis plot quantified their effects. This combined statistical and biological approach clarified how CO_2 concentration, light intensity, photoperiod, and nitrogen content modulate growth, protein production, and CO_2 fixation, providing a robust strategy to optimize microalgae performance for single-cell protein and carbon biofixation applications.

Table 2: Summary of the results obtained from the Taguchi OA design

	Factor A	Factor B	Factor C	Factor D	Resp. 1	Resp. 2	Resp. 3	Resp. 4
Run	**CO_2 conc. (%)**	**Light int. (kLx)**	**Light period (hr)**	**Nitrogen cont. (g/L)**	**Growth rate (day^{-1})**	**CO_2 capture (%)**	**Protein prod. (g/g/day)**	**Lipid cont. (%)**
1	3	15	8	0.05	0.189	14.04	0.057	22.00
2	1	10	12	0.05	0.135	39.68	0.020	20.00
3	1	15	16	0.10	0.140	20.82	0.018	13.00
4	1	5	8	0.00	0.097	12.00	0.034	25.00
5	3	10	16	0.00	0.067	27.41	0.013	15.00
6	3	5	12	0.10	0.222	15.00	0.046	19.00
7	5	15	12	0.00	0.095	93.19	0.025	17.91
8	5	10	8	0.10	0.469	20.47	0.009	4.39
9	5	5	16	0.05	0.048	87.42	0.004	93.57

3.2. Effect of the Selected Parameters on the Growth Rate

The effects of CO_2 concentration, light intensity, light period, and nitrogen content on *C. vulgaris* growth were assessed using half-normal plots, ANOVA, and one-factor analysis plots. The half-normal plot is a graphical tool used to visually assess the significance of factors in a designed experiment. It plots the absolute values of the estimated effects of each factor against a cumulative normal probability scale. In this plot, effects that lie close to the reference line are generally considered insignificant, as they fall within the range expected due to random variation (noise). In contrast, factors that deviate markedly from the line are likely to be significant contributors to the response variable. In this study, the half-normal plot (Fig. 5) identified nitrogen content (factor D) as the most dominant variable, followed

by light period (factor C). Light intensity (factor B) appeared closer to the reference line, suggesting a weaker contribution, whereas CO_2 concentration (factor A) was effectively inert in influencing growth rate in this model.

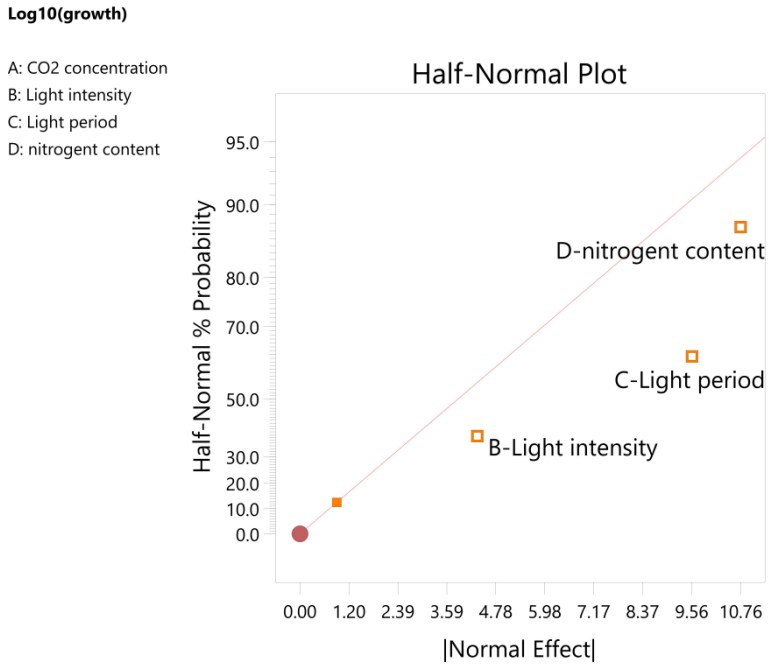

Fig. 5. Half-normal plot of significant factors for Response 1: growth rate (day^{-1})

These graphical trends were quantitatively supported by ANOVA (Table 3), which confirmed nitrogen content ($p = 0.0163$; $F = 60.48$) and light period ($p = 0.0203$; $F = 48.30$) as statistically significant factors at the 5% confidence level. Light intensity ($p = 0.0826$, $F=11.11$) exhibited a moderately significant effect, and the overall model fit was robust, as indicated by a significant F-value (39.96) and a p-value of 0.0246 ($p < 0.05$), confirming the model's validity. The high predicted R^2 value of 0.8325 indicates a small gap between adjusted and predicted R^2 (less than 0.2), further reinforcing the predictive accuracy and reliability of the regression model.

The equation obtained in terms of coded factors for the growth rate of *C. vulgaris* (Eq. (15)) indicates that moderate light intensity(B), shorter light period(C), and higher nitrogen content (D) provide a higher growth rate.

$$Log_{10}(growth) = -0.8839 - 0.1109 \times B[1] + 0.0931 \times B[2] + 0.1954 \times C[1] + 0.1954 \times C[2] - 0.1859 \times D[1] - 0.0861 \times D[2] \quad (15)$$

These trends align closely with the one-factor analysis plots (Fig.6) which showed that CO_2 concentration at all levels (no effect), level 2 of B (Light intensity: 10 kLx), level 1 of C (Light period: 8 hr), and level 3 of D (Nitrogen concentration: 0.1 g/L-N), give a higher growth rate.

Table 3: ANOVA analysis of the growth rate (day^{-1})

Source	Sum of Squares	df	Mean Square	*F-value*	*p-value*	
Model	0.6894	6	0.1149	39.96	0.0246	**significant**
B	0.0639	2	0.0319	11.11	0.0826	
C	0.2777	2	0.1389	48.30	0.0203	
D	0.3478	2	0.1739	60.48	0.0163	
Residual	0.0058	2	0.0029			
Cor Total	0.6952	8				

Note. R^2= 0.9917 *Adj* –R^2= 0.9669, *Pred* –R^2= 0.8325

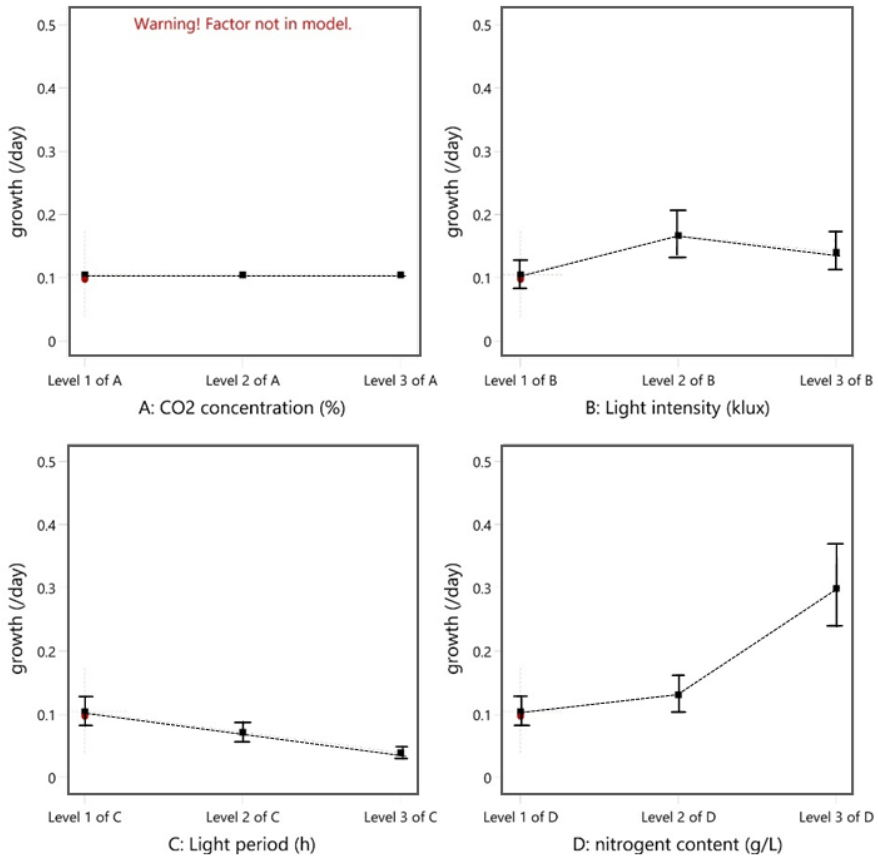

Fig. 6. One-factor analysis graph of the significant variables of growth rate (day^{-1})

Interestingly, CO_2 concentration did not significantly affect the specific growth rate (μmax) across the tested levels. This aligns with findings by Jose et al. (2016) [25],who reported minimal growth differences in *C. vulgaris* when CO_2 varied between 0.04% and 5.2%, likely due to the culture pH remaining stable between 6 and 8. In our study, after 30 minutes of sparging, pH increased gradually (7–9), indicating that CO_2 uptake by cells exceeded supply. This is consistent with *C. vulgaris*'s robust carbon-concentrating

mechanism (CCM) that efficiently captures both gaseous CO_2 and dissolved inorganic carbon (HCO_3^-)[26,27] This efficient carbon assimilation likely explains the lack of CO_2 effect on growth within the tested range.

In contrast, nitrogen concentration, light period, and light intensity showed a strong interdependent influence on growth. Nitrogen was the most critical factor, essential for protein synthesis, chlorophyll production, and cell division, thus directly supporting biomass accumulation. However, its positive effect was modulated by light conditions. Shorter photoperiods favor higher growth rates, as prolonged illumination can cause photoinhibition or oxidative stress that diminishes photosynthetic efficiency. Light intensity exhibited a non-linear relationship: moderate intensities (e.g., 10 kLx) enhanced growth, but higher levels (15 kLx) likely exceeded the light saturation point of *C. vulgaris*, causing photoinhibition and reduced productivity [7].

These effects are tightly linked. Under nitrogen-limited conditions, excessive light, whether by intensity or duration, accelerates nutrient consumption without a corresponding increase in biomass, leading to metabolic stress. This was demonstrated by the highest growth rate (0.469 day^{-1}) at moderate light intensity (10 kLx), short photoperiod (8 hours), and high nitrogen (0.1 g/L-N) (Run 8, Table 2), while increasing light or photoperiod without sufficient nitrogen caused sharp growth declines (0.067 day^{-1} in Run 5 and 0.048 day^{-1} in Run 9; Table 1). Such findings highlight the importance of balancing nutrient supply and light exposure, as emphasized in prior studies.

In summary, *C. vulgaris* tolerates a wide range of CO_2 levels due to its effective CCM, but optimal growth depends on the synergistic balance of nitrogen availability and controlled light conditions. Managing moderate light intensity and shorter photoperiods alongside sufficient nitrogen supply prevents photoinhibition and nutrient exhaustion, maximizing microalgal productivity. These insights are critical for optimizing process parameters to ensure efficient growth and resource use.

3.3. Effect of the Selected Parameters on the CO_2 Capture

The influence of cultivation conditions on CO_2 capture by *C. vulgaris* revealed a distinct pattern from that observed for growth rate. As shown in the half-normal plot (Fig.7), CO_2 concentration (factor A) emerged as the most significant driver of carbon uptake, followed by light period (factor C) and nitrogen content (factor D). Light intensity (factor B), while essential for photosynthesis, appeared to have minimal direct influence on CO_2 capture under the tested conditions.

These trends were quantitatively supported by ANOVA (Table 4). With a CO_2 concentration showing a highly significant effect ($F = 42.31$; $p = 0.0231$), Taguchi suggests that increasing gas-phase CO_2 enhances the net dissolution into the medium during cultivation and the cell's ability to fix inorganic carbon. The statistical strength of the model was confirmed by a high overall F-value (29.71) and a low p-value (< 0.05), indicating that the observed effects are unlikely to be due to random variation. The probability of obtaining such a high model F-value by chance was only 3.29%, further reinforcing its reliability.

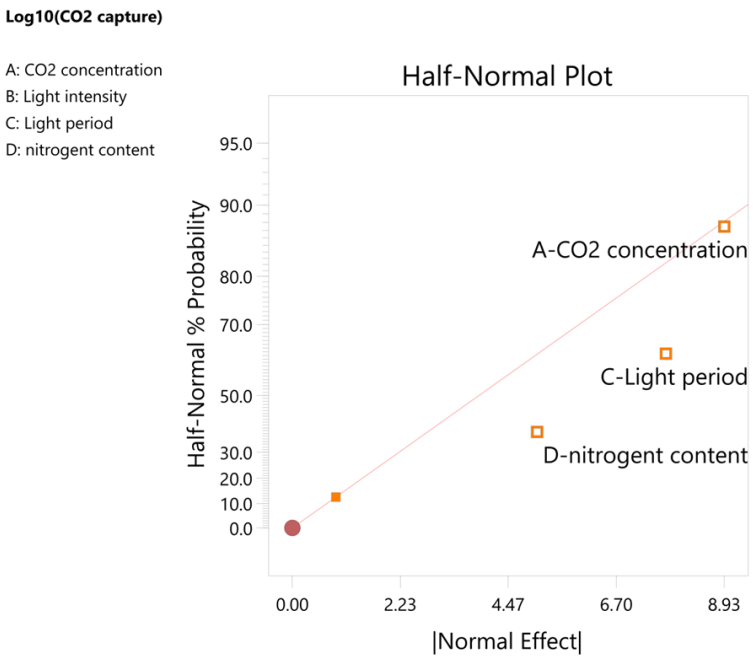

Fig. 7. Half-normal plot of the significant factors for Response 2 of CO_2 capture (%)

Table 4: ANOVA analysis of the CO_2 capture (%)

Source	Sum of Squares	df	Mean Square	*F-value*	*p-value*	
Model	0.8640	6	0.1440	29.71	0.0329	significant
A-CO_2 concentration	0.4102	2	0.2051	42.31	0.0231	
C-Light period	0.3114	2	0.1557	32.12	0.0302	
D-nitrogen content	0.1424	2	0.0712	14.69	0.0637	
Residual	0.0097	2	0.0048			
Cor Total	0.8737	8				

R^2= 0.989, *Adj* –R^2= 0.956, *Pred* –R^2= 0.775

The regression equation in coded terms (Eq. (16)) suggests that increased CO_2 concentration (A2), a moderate light period (C2), and a higher nitrogen content (D2) favor enhanced CO_2 capture. This trend is clearly reflected in the main-effect plot (Fig.8), which shows a distinct upward trajectory in CO_2 capture at higher CO_2 concentrations, contrasting with its negligible effect on growth rate. Higher CO_2 concentration provides higher CO_2 capture under a light period of 12 hr and nitrogen concentration of 0.05g/L-N (Level 2). These results highlight how the optimal conditions for CO_2 capture efficiency differ from those promoting biomass growth, emphasizing the importance of tailoring operational parameters to specific cultivation objectives.

$$Log^{10}(CO_2\ capture) = +1.44 - 0.1101 \times A[1] - 0.1884 \times A[2] - 0.2629 \times C[1] + 0.1391 \times C[2] + 0.0533 \times D[1] + 0.1204 \times D\ [2] \quad (16)$$

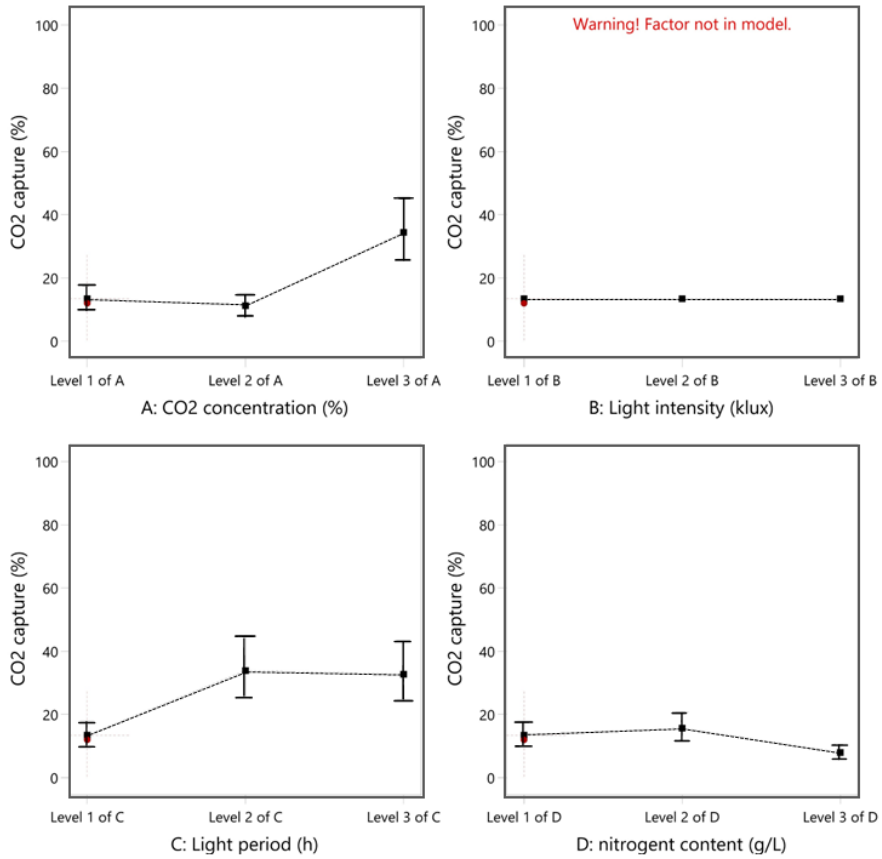

Fig. 8. One-factor analysis graph of the significant variables of the CO_2 capture (%)

The biological rationale behind these Taguchi trends lies primarily in the CO_2/O_2 competition mechanism within the Calvin–Benson cycle. Indeed, the ratio of CO_2 to O_2 in the environment plays a crucial role in determining whether microalgae engage in photosynthesis (carboxylation) or photorespiration (oxygenation), as highlighted by[7,28]. When CO_2 levels are significantly low, the enzyme Rubisco, which is vital for the Calvin cycle, tends to favor its oxygenase function; This shift hinders effective CO_2 capture. In contrast, when CO_2 concentrations are high, Rubisco's carboxylase activity is enhanced, facilitating CO_2 fixation and subsequently leading to the production of carbonic anhydrase (CA).

Longer exposition of the culture to light sources also affects the CO_2/O_2 mechanism, as it increases the release of O_2, leading to an inhibition of the Calvin-Benson cycle and the release of CO_2 [29]. Chunzhuk et al. (2023) [30] highlighted that light intensity highly affects the capture by the microalgae. He shows that higher intensity gives better growth and CO_2 capture. However, it is important to note that the photoperiod was maintained for 24 hr, and the light intensity was lower than in our study (80-240 µmol/m^2/s). Thus, no photoinhibition occurred as the light intensity was a limiting source.

The correlation between nitrogen assimilation and carbon capture lies in their influence on microalgae growth, metabolism, and adaptation to environmental changes. When nitrogen is abundant, microalgae can multiply and support high rates of photosynthesis. However, when nitrogen is limited, algae often undergo metabolic changes such as

increased storage of carbohydrates or lipids [31]. For example, under nitrogen limitation, the microalgae may prioritize energy production and survival by activating their CCM to maximize carbon fixation, even in low CO_2 conditions [32]. This increased concentration of CO_2 around Rubisco helps maintain photosynthetic efficiency despite nitrogen limitation. This adaptive mechanism explains why higher CO_2 capture (87.42%) was observed at mild nitrogen levels (e.g., run 9 with 0.05g L^{-1} N), which also coincided with elevated lipid accumulation (93.57%).

In summary, the Taguchi trends suggest that the optimal biological conditions for maximizing CO_2 capture in freshwater *C. vulgaris* involve a moderately high CO_2 concentration, a 12-hour photoperiod, and low-to-moderate nitrogen availability. These conditions collectively enhance Rubisco carboxylation efficiency, maintain photosystem stability, and stimulate the carbon-concentrating mechanism, thereby promoting efficient CO_2 fixation. The findings confirm that optimizing CO_2/O_2 dynamics and nutrient supply, rather than merely increasing light or nitrogen input, is crucial for improving carbon capture performance in photobioreactor cultivation of *C. vulgaris.*

3.4. Effect of the Selected Parameters on the Protein Productivity

The effect of cultivation parameters on *C. vulgaris* protein productivity was analyzed using Taguchi design, incorporating half-normal plots, ANOVA, regression modeling, and one-factor-at-a-time response plots. The half-normal plot (Fig. 9) identified the light period (C) as the most influential variable, followed by CO_2 concentration (A) and light intensity (B). Factors positioned farther from the reference line represent stronger effects on the response, indicating that the light regime plays a predominant role in determining protein productivity in *C. vulgaris*. The remaining factor, nitrogen content, was close to the line and excluded from the model due to its negligible effect, likely because the nitrogen range tested was sufficient to sustain metabolic demand without becoming growth-limiting.

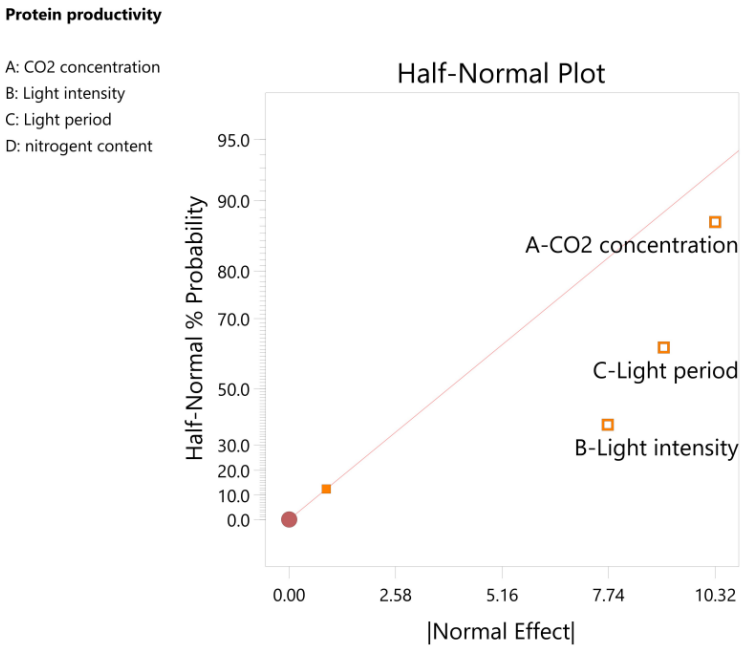

Fig.9. Half-normal plot of the significant factors for Response 3: protein productivity (g/g/day)

The ANOVA results (Table 5) corroborated these graphical findings, confirming that all included factors were statistically significant at the 5% confidence level: CO_2 concentration ($p = 0.0176$, $F = 55.86$), light intensity ($p = 0.0302$, $F = 32.09$), and light period ($p = 0.0224$, $F = 43.65$). The model exhibited high reliability ($R^2 = 0.993$; Adj-$R^2 = 0.997$; Pred-$R^2 = 0.847$), demonstrating an excellent fit between experimental and predicted values. This strong agreement indicates that the selected parameters sufficiently explain the variability in protein productivity, validating the Taguchi design as an efficient optimization approach.

Table 5: ANOVA analysis of protein productivity (g/g/day)

Source	Sum of Squares	df	Mean Square	*F-value*	*p-value*	
Model	0.0024	6	0.0004	43.87	0.0225	**significant**
A	0.0010	2	0.0005	55.86	0.0176	
B	0.0006	2	0.0003	32.09	0.0302	
C	0.008	2	0.0004	43.65	0.0224	
Residual	0.000	2	9.260E-06			
Cor Total	0.0025	8				

R^2= 0.993, *Adj* $-R^2$= 0.997, *Pred* $-R^2$= 0.847

The regression equation (Eq. (17)) derived from the model reveals that intermediate CO_2 (A2), low-to-moderate light intensity (B1), and shorter light periods (C1–C2) exert positive effects on protein productivity. These trends align closely with the one-factor analysis plots (Fig.10), which illustrate that protein productivity peaked at the mid-level of CO_2 concentration (Level 2), moderate light intensity (Level 1–3), and shorter photoperiods. Nitrogen content showed minimal variation across levels, confirming its statistical insignificance in this range.

$$Protein\ productivity = +0.0250 - 0.0012 \times A[1] + 0.0137 \times A[2] + 0.0027 \times B[1] - 0.0110 \times B[2] + 0.0082 \times C[1] + 0.0051 \times C[2] \quad [17]$$

Nitrogen plays a central role in microalgal physiology, as it supports essential processes like protein synthesis, cell division, and biomass formation. Typically, increased nitrogen availability is associated with higher growth and protein content due to its role in amino acid and enzyme production. However, in this study, nitrogen source had a less pronounced effect on protein content than expected, contrasting with findings that identify nitrogen as a primary driver of protein synthesis [7,13].

This discrepancy may be explained by the nitrogen concentration range used, which fell within previously identified optimal levels [7,14,15]. Within such a range, changes in nitrogen type or amount may have limited impact, as the cells are not under nutrient stress. Additionally, in nitrogen-rich environments, microalgae often prioritize rapid cell proliferation over protein accumulation, reallocating nitrogen toward structural growth or

nucleic acid synthesis rather than protein production. This can lead to a lower protein-to-biomass ratio, even as total biomass increases [16].

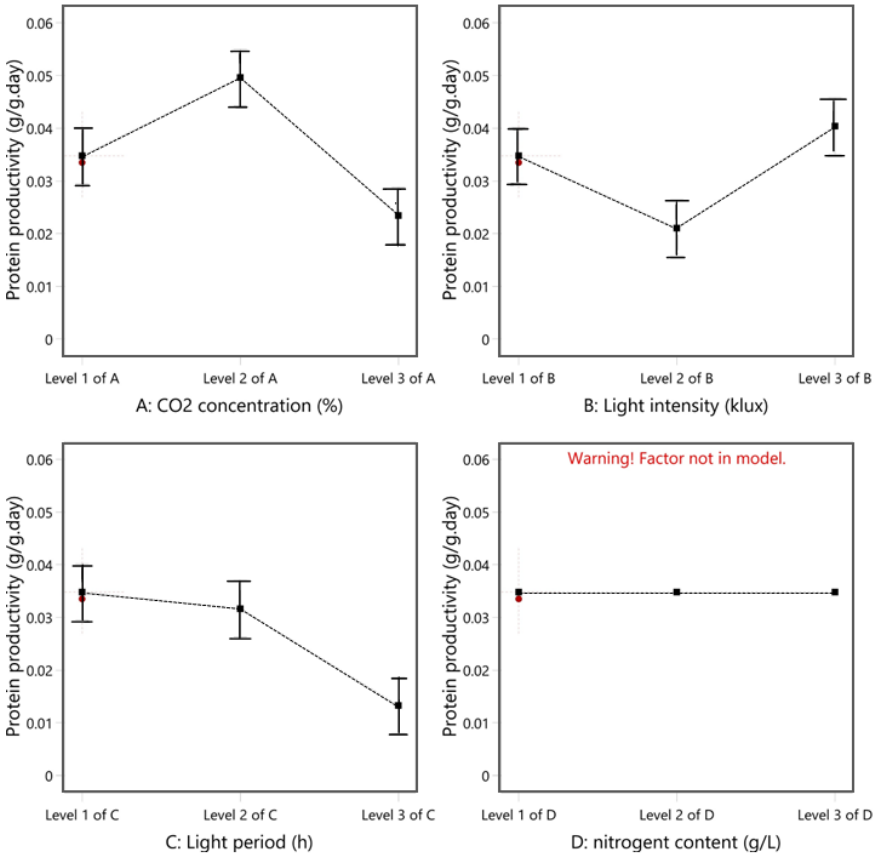

Fig.10. One-factor analysis graph of the significant variables of protein productivity (g/g/day)

Light conditions also influenced protein content, though differently than for growth. While excessive light intensity can lead to photoinhibition and lower productivity, moderate to high intensities are generally more favorable for protein synthesis, provided that photoperiod is properly managed. Past studies have shown that low-intensity light (<2 kLx) triggers metabolic pathways favoring amino acid synthesis, while overly intense light (>17 kLx) suppresses both protein and biomass yields due to oxidative stress [6,7]. In this study, the use of high light intensity paired with a shorter light period likely helped mitigate such effects, resulting in protein yields (0.05–0.13 g/L) consistent with values reported in the literature [5,17]. Overall, *C. vulgaris* demonstrated robust protein biosynthesis efficiency even under sub-optimal growth conditions, confirming its potential for sustainable SCP production.

3.5.Validation of the Model

To evaluate the predictive power of the Taguchi optimization and assess trade-offs between different performance metrics, three experimental conditions (V1, V2, and V3) were selected for validation in 2-L borosilicate bottle photobioreactors (PBRs). Each run reflected a different optimization strategy: V1 targeted a balanced outcome across growth rate, CO_2 capture, and protein productivity; V2 prioritized CO_2 capture efficiency, while V3

focused on maximizing protein productivity (Table 6). This selection enabled a comparative analysis of single-objective versus multi-objective optimization outcomes, a strategy supported in prior microalgal studies [11,13,33] .

Table 6: Numerical optimization design obtained from the Taguchi OA analysis

Parameters/ Responses	V1: all responses (S.B)	V2: CO_2 capture (S.B)	V3: Protein Productivity (S.B)
CO_2 concentration (%)	1	5	1
Light intensity (kLx)	5	15	15
Light period (hr)	12	12	16
Nitrogen content (g/L)	0.05	0.05	0.05
Growth rate (/day)	0.091	0.097	0.122
CO_2 capture (%)	39.55	86.84	38.17
Protein productivity (g/g/day)	0.032	0.026	0.037
Desirability	0.828	0.807	0.809

S.B = 2-L glass bottle photobioreactor

The experimental results closely matched the predicted values generated by the Taguchi model, with deviation percentages ranging between 2% and 10% for all measured responses (Table 7). Such variation is well within acceptable limits for biological systems, where minor environmental fluctuations and physiological variability are expected [13]. Growth rate predictions deviated by 6–8%, while protein productivity demonstrated particularly high predictive accuracy, with only a 2% difference in V1. These results reinforce the model's reliability in estimating biomass and protein outputs, especially under nitrogen- and light-regulated growth conditions.

Table 7: Summary of predicted and experimental results for model validation

Variables	Experiment	Predicted	Δ%
Growth rate (/day)	V1	0.091	6
	V2	0.097	8
	V3	0.122	7
CO_2 capture (%)	V1	39.55	7
	V2	86.84	8
	V3	39.55	21
Protein productivity (g/g/day)	V1	0.032	2
	V2	0.026	10
	V3	0.037	4

However, greater variability was observed in CO_2 capture, particularly in V3, where the experimental capture rate exceeded predictions by 21%. This discrepancy may reflect unmodeled influences such as gas-liquid mass transfer efficiency or intracellular carbon partitioning, which are known to complicate CO_2 utilization in dense cultures [28]. This suggests that while statistical optimization offers strong predictive capacity for intracellular metrics like protein content, extracellular parameters such as CO_2 removal may be more sensitive to reactor dynamics and aeration regimes.

Performance comparisons among the three runs further underscore the importance of response prioritization in multi-objective bioprocess optimization. V3, for instance, produced the highest growth rate (0.113 day^{-1}) and protein productivity (0.035 g/g/day), affirming the efficacy of its parameter set for maximizing SCP yield. Conversely, V2, although achieving the highest CO_2 capture (79.7%), exhibited lower biomass and protein accumulation, reaffirming earlier findings that elevated CO_2 supply can enhance uptake but does not guarantee proportional conversion into biomass or metabolites [24,34]. This highlights a common trade-off in microalgae-based carbon capture systems: optimizing gas removal may not align with maximizing cellular biosynthesis.

Overall, these findings validate the Taguchi model as a robust framework for multi-response optimization in microalgal cultivation. More importantly, they emphasize the need to tailor optimization strategies based on desired application; whether prioritizing environmental remediation through CO_2 sequestration or enhancing protein yields for SCP applications. The combined evaluation of growth, capture efficiency, and protein content thus provides a comprehensive understanding of how environmental parameters influence both cellular metabolism and system-level performance.

3.6. CO_2 Utilization Performance and PBR Design

To evaluate CO_2 utilization strategies, three optimized Schott bottle cultivations (V1–V3) were compared based on growth, protein productivity, and carbon capture metrics (Table 8). Among these, V3, optimized for protein yield, achieved the highest biomass productivity (0.029 g/L/day), growth rate (0.113 day^{-1}), and CO_2 fixation efficiency (6.61%), suggesting that nutrient-driven metabolism, particularly enhanced nitrogen availability, plays a central role in improving both protein synthesis and carbon assimilation [8,35]. In contrast, V2 showed the highest CO_2 capture (96.7%) but low fixation efficiency (0.80%), highlighting a disconnect between CO_2 uptake and actual metabolic incorporation. This decoupling supports previous findings that elevated CO_2 can lower pH and inhibit carbonic anhydrase activity, thus limiting fixation despite high dissolved CO_2 [26]. These observations emphasize the importance of balancing nutrient and gas inputs, as maximizing CO_2 uptake alone does not ensure higher productivity.

When the same optimized condition (V1) was applied in a flat-panel photobioreactor (V4), a notable improvement in all performance metrics was observed. V4 outperformed all Schott bottle runs, doubling biomass productivity (0.035 g/L/day) and increasing CO_2 fixation efficiency by over 35% compared to the best bottle-based result (V3). These improvements can be attributed to enhanced reactor geometry and mass transfer characteristics of flat-panel designs. Specifically, these PBRs offer a higher surface-to-volume ratio, enabling more uniform light distribution, superior gas-liquid contact, and better mixing, all of which support sustained photosynthetic activity and reduce limitations such as oxygen accumulation or CO_2 stratification [17]. The ability of V4 to simultaneously

support high biomass production and CO_2 fixation suggests that reactor design plays a decisive role in unlocking the full potential of parameter optimization.

Table 8: Chemical characteristics of the *C.vulgaris* from the optimized conditions

No. Run	V1 (max all)	V2 (CO_2 capture)	V3 (Protein)	V4 (PBR) (max all)
Gas flow conditions	0.8vvm 1% CO_2 for 30 min daily	0.8 vvm 5% CO_2 for 30 min daily	0.8vvm 1% CO_2 for 30 min daily	0.8vvm 1% CO_2 for 30 min daily
Maximum optical density at 680 nm (A)	1.567 (day 12)	1.379 (day 12)	1.299 (day 13)	1.709 (day13)
Maximum biomass productivity, P_{max} (g/L/day)	0.018	0.017	0.029	0.035
Maximum growth rate, μ_{max} (day^{-1})	0.086	0.089	0.113	0.127
Maximum CO_2 capture (%)	75.179	96.722	81.554	87.974
Maximum CO_2 fixation rate (g/L/day)	0.016	0.019	0.031	0.043
Maximum CO_2 fixation efficiency (%)	3.316	0.796	6.612	9.049

Despite the relative improvements seen in V4, the absolute growth and CO_2 fixation rates remain lower than those reported in other studies using *C. vulgaris* under continuous CO_2 supply or higher light intensities. Literature values often exceed 0.2 day^{-1} for growth and 0.1 g/L/day for fixation under more intensive operational regimes [3,24,34,36,37]. This variation likely arises from differences in reactor scale, CO_2 dosing strategy, light spectra, and strain-specific responses. However, the consistent trends observed across conditions confirm the internal validity of the optimization approach used here and suggest that further enhancements may be achieved through continuous CO_2 delivery, improved light regimes, or adaptive cultivation strategies.

3.7. Kinetic Growth Study

To evaluate growth dynamics across the optimized runs (V1–V4), kinetic modeling from Origin Pro v25 was performed using the Logistic, Monod, and Gompertz models (Table 9). Among these, the Logistic model provided the best fit, with R^2 values ranging from 0.625 to 0.931 (Table 9 and Fig. 11), indicating strong alignment with the observed S-shaped growth patterns typical under well-optimized conditions. This suggests that cell proliferation in these systems was initially exponential but gradually slowed as resource limitations approached the culture's carrying capacity; a dynamic well captured by the logistic framework. Such behavior has been widely reported in microalgal cultivation where environmental parameters (e.g., light, nitrogen, and CO_2) are sufficiently optimized [20–22]. However, some studies, such as Meng & Kassim (2020) [24], report better performance using the Gompertz model, these discrepancies are likely linked to species-specific physiology and media composition [23]. The strong fit observed here underscores that the

logistic model is particularly suited to describe *C. vulgaris* growth under the balanced and resource-rich conditions established in the present study.

Table 9: R^2 of the different kinetic models obtained from Origin Pro v25

Model used	**Reference for growth rate**	R^2 **(Levenberg Marquardt)**			
		V1	**V2**	**V3**	**V4**
Logistic	Meng & Kassim, (2020)	0.798	0.813	0.802	0.429
	Azmi et al. (2020)	0.608	0.799	0.8034	0.933
	Taguchi OA (our study)	0.625	0.818	0.802	0.931
Multiplicative	Romagnoli et al., 2021	no fitting	no fitting	no fitting	no fitting
Gompertz	Meng & Kassim, (2020)	no fitting	no fitting	no fitting	no fitting

While the logistic model provided the best statistical fit among the tested growth models, some limitations became evident when comparing predicted and experimental values (Table 10). The relatively lower correlation coefficients (e.g., R^2 = 0.625 for V1) and the overestimation of maximum biomass concentrations (X_{max}) suggest that the classical logistic formulation may oversimplify growth dynamics under multi-factorial influences. Unlike the logistic model derived from previous studies [22,24] which relied on fixed growth rate constants derived from past data, the present study used growth rates generated from Taguchi orthogonal array (OA) analysis; an approach that accounts for interactive effects of light, nitrogen, and CO_2 assimilation. This integrated method likely contributed to improved model fitting in some runs, particularly V4 (R^2 = 0.931), but also exposed the logistic model's inherent limitation: its inability to consider substrate-dependent growth or time-based nutrient depletion. In practice, X_{max} values predicted by the model assume biomass accumulation continues until full carrying capacity is reached, which may require cultivation periods longer than the experimental duration (14 days). This disconnect is visible in Fig. 11, where most runs had not yet reached the stationary phase, indicating that the model may better reflect potential rather than actual outcomes within the tested timeframe.

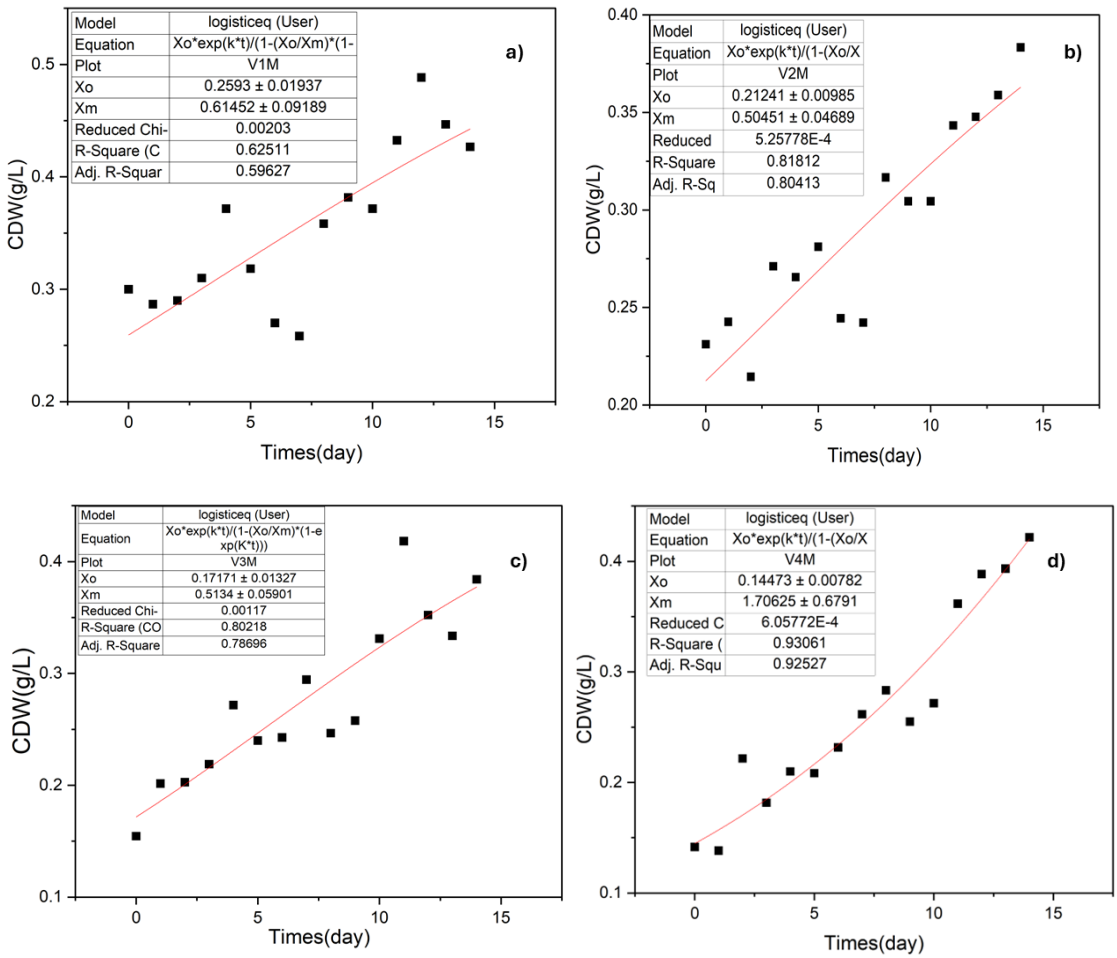

Fig.11. Growth curve of *C. vulgaris* under various conditions: a) V1: all responses (S. B), b) V2: CO_2 (S. B), c) V3: Protein (S. B), and d) V4: all responses (PBR)

Table 10: Summary of the kinetic growth curve validation

Run	Parameters predicted by the model				Parameters from the experimental data		
	R^2	X_{max} (g/L)	X_o (g/L)	μ_{max} (day^{-1})	X_{max}(g/L)	X_o (g/L)	μ_{max} (day^{-1})
V1 (a)	0.625	0.615	0.259	0.091	0.488	0.300	0.086
V2 (b)	0.818	0.505	0.212	0.091	0.383	0.231	0.089
V3 (c)	0.802	0.513	0.171	0.121	0.418	0.154	0.113
V4 (d)	0.931	1.706	0.144	0.091	0.421	0.141	0.127

Further interpretation of chemical data (Table 11) supports this view. Runs with closer alignment between predicted and experimental biomass values show better carbon and nitrogen assimilation. Particularly, V4, the run conducted in the airlift PBR, which also exhibited the best data fit ($R^2 = 0.931$), also recorded the highest CO_2 fixation (9.05%) and nitrogen efficiency (84.97%). In contrast, runs like V1 and V2, which exhibited larger discrepancies, have lower nitrogen fixation efficiencies (46.36% and 50.53%, respectively), suggesting that suboptimal substrate uptake limited actual growth. These findings align with [20,38] which emphasized the central role of substrate assimilation in shaping growth kinetics. While the Taguchi approach effectively isolated major contributing factors, it did not include variables such as nutrient saturation or inhibition thresholds, nor did it account for temperature variation, despite its known influence on enzymatic activity and growth rate. Hence, it can be seen that both nitrogen fixation efficiency and carbon fixation efficiency fell below the optimum values reported in previous studies [15,39,40]. The ideal nitrogen and carbon fixation efficiencies are expected to be above 90% and 10%, respectively. Taken together, these findings highlight both the strengths and limitations of current modeling approaches. The logistic model, when coupled with empirically derived growth rates, offers a useful approximation of biomass trends but may overestimate growth under non-ideal or resource-limited conditions.

Table 11: Summary of the chemical characteristics of the optimum runs

No. Run	V1 (max all)	V2 (CO_2 capture)	V3 (Protein)	V4 (PBR) (max all)
Gas flow conditions	0.8 vvm 1% CO_2 for 30 min daily	0.8 vvm 5% CO_2 for 30 min daily	0.8 vvm 1% CO_2 for 30 min daily	0.8 vvm 1% CO_2 for 30 min daily
Maximum CO_2 capture (%)	75.179	96.722	81.554	87.974
Maximum CO_2 fixation efficiency (%)	3.316	0.796	6.612	9.049
Maximum carbon content (%)	24.148	28.984	29.146	33.729
Maximum nitrogen content (%)	4.75	5.59	5.123	7.325
Maximum Nitrogen fixation (%)	46.36	50.533	57.787	84.97
Maximum protein content (%)	29.688	34.938	32.019	45.781
Maximum lipid content (%)	29.969	27.966	5.536	44.279

4. CONCLUSION

The use of the Taguchi Orthogonal Array successfully optimized the cultivation conditions for *C. vulgaris*, resulting in a maximum CO_2 capture of 93.19% and protein productivity of 0.057 g/g/day. All modelled responses were statistically significant ($p < 0.05$), with validation runs showing less than 10% deviation from predicted values, confirming the robustness of the optimization approach. Cultivation in a 2 L flat panel photobioreactor under optimized conditions further improved biomass concentration and

biochemical quality, demonstrating the importance of reactor design in enhancing productivity. Kinetic modelling showed that the logistic growth model, fitted using Taguchi-derived growth rates, best described the growth dynamics ($R^2 = 0.60–0.93$), outperforming alternative models. Future work should explore continuous cultivation with real-time CO_2 control to enhance long-term productivity, as well as strain-level metabolic profiling to gain deeper insight into carbon assimilation and protein synthesis mechanisms. Additionally, evaluating the optimized process in a scaled-up system using industrial CO_2 sources will help assess scalability and operational stability. A techno-economic analysis would further support the development of *C. vulgaris* as a viable platform for sustainable protein production and carbon capture.

ACKNOWLEDGEMENT

The authors thank PETRONAS Research Sdn. Bhd (PRSB) for its financial support through PACD Cycle 1 (SPP22-122-0122).

REFERENCES

[1] Li, G., Xiao, W., Yang, T. and Lyu, T. (2023) Optimization and Process Effect for Microalgae Carbon Dioxide Fixation Technology Applications Based on Carbon Capture: A Comprehensive Review. *C 2023, Vol 9, Page 35*, Multidisciplinary Digital Publishing Institute. **9**, 35. https://doi.org/10.3390/C9010035

[2] Janssen, M., Wijffels, R.H. and Barbosa, M.J. (2022) Microalgae based production of single-cell protein. Curr Opin Biotechnol. Elsevier Ltd. https://doi.org/10.1016/j.copbio.2022.102705

[3] Iglina, T., Iglin, P. and Pashchenko, D. (2022) Industrial CO2 Capture by Algae: A Review and Recent Advances. Sustainability (Switzerland). MDPI. https://doi.org/10.3390/su14073801

[4] Kang, S., Heo, S. and Lee, J.H. (2019) Techno-economic Analysis of Microalgae-Based Lipid Production: Considering Influences of Microalgal Species. *Industrial and Engineering Chemistry Research*, American Chemical Society. **58**, 944–55. https://doi.org/10.1021/ACS.IECR.8B03999/ASSET/IMAGES/MEDIUM/IE-2018-03999D_0007.GIF

[5] Barros de Medeiros, V.P., da Costa, W.K.A., da Silva, R.T., Pimentel, T.C. and Magnani, M. (2022) Microalgae as source of functional ingredients in new-generation foods: challenges, technological effects, biological activity, and regulatory issues. Crit Rev Food Sci Nutr. Taylor and Francis Ltd. p. 4929–50. https://doi.org/10.1080/10408398.2021.1879729

[6] Thiviya, P., Gamage, A., Kapilan, R., Merah, O. and Madhujith, T. (2022) Single Cell Protein Production Using Different Fruit Waste: A Review. Separations. MDPI. https://doi.org/10.3390/separations9070178

[7] Maltsev, Y., Maltseva, K., Kulikovskiy, M. and Maltseva, S. (2021) Influence of Light Conditions on Microalgae Growth and Content of Lipids, Carotenoids, and Fatty Acid Composition. *Biology 2021, Vol 10, Page 1060*, Multidisciplinary Digital Publishing Institute. **10**, 1060. https://doi.org/10.3390/BIOLOGY10101060

[8] Nordin, N., Yusof, N., Md Nadzir, S., Mohd Yusoff, M.Z. and Hassan, M.A. (2022) Effect of photo-autotrophic cultural conditions on the biomass productivity and composition of

Chlorella vulgaris. *Biofuels*, Taylor and Francis Ltd. **13**, 149–59. https://doi.org/10.1080/17597269.2019.1652787

[9] Feng, J. and Qian, S. (2023) Accelerating autonomic healing of cementitious composites by using nano calcium carbonate coated polypropylene fibers. *Materials and Design*, Elsevier Ltd. **225**. https://doi.org/10.1016/j.matdes.2022.111549

[10] Shekh, A., Sharma, A., Schenk, P.M., Kumar, G. and Mudliar, S. (2022) Microalgae cultivation: photobioreactors, CO2 utilization, and value-added products of industrial importance. Journal of Chemical Technology and Biotechnology. John Wiley and Sons Ltd. p. 1064–85. https://doi.org/10.1002/jctb.6902

[11] Davis, R. and John, P. (2018) Application of Taguchi-Based Design of Experiments for Industrial Chemical Processes. *Statistical Approaches With Emphasis on Design of Experiments Applied to Chemical Processes*,. https://doi.org/10.5772/intechopen.69501

[12] Al-Rikabey, M.N. (2018) Experimental Design of Chlorella Vulgaris Cultivation in Wastewater of Al-rustamiyah South Station. *Available Online WwwJocprCom Journal of Chemical and Pharmaceutical Research*, **10**, 35–43.

[13] Tharek, A., Yahya, A., Salleh, M.M., Jamaluddin, H., Yoshizaki, S., Dolah, R. et al. (2020) Improvement of astaxanthin production in coelastrum sp. by optimization using taguchi method. *Applied Food Biotechnology*, **7**. https://doi.org/10.22037/afb.v7i4.29697

[14] Al-Mayah, A.M., Naeemah, M. and Al-Rikabey, M.N. (2018) Cultivation of Chlorella Vulgaris in BG-11 Media Using Taguchi Method [Internet]. Article in Journal of Advanced Research in Dynamical and Control Systems.

[15] Paladino, O. and Neviani, M. (2024) Interchangeable modular design and operation of photo-bioreactors for Chlorella vulgaris cultivation towards a zero-waste biorefinery. *Enzyme and Microbial Technology*, Elsevier Inc. **173**. https://doi.org/10.1016/j.enzmictec.2023.110371

[16] Rahman, M.R. and Hellgardt, K. (2025) Flat-plate photobioreactors for renewable resources production. *Algal Bioreactors: Science, Engineering and Technology of Upstream Processes: Volume 1*, Elsevier Science Ltd. **1**, 423–47. https://doi.org/10.1016/B978-0-443-14058-7.00019-1

[17] Abdur Razzak, S., Bahar, K., Islam, K.M.O., Haniffa, A.K., Faruque, M.O., Hossain, S.M.Z. et al. (2024) Microalgae cultivation in photobioreactors: sustainable solutions for a greener future. Green Chemical Engineering. https://doi.org/10.1016/j.gce.2023.10.004

[18] Romagnoli, F., Weerasuriya-Arachchige, A.R.P.P., Paoli, R., Feofilovs, M. and Ievina, B. (2021) Growth Kinetic Model for Microalgae Cultivation in Open Raceway Ponds: A System Dynamics Tool. *Environmental and Climate Technologies*, Sciendo. **25**, 1317–36. https://doi.org/10.2478/RTUECT-2021-0100

[19] Lee, E., Jalalizadeh, M. and Zhang, Q. (2015) Growth kinetic models for microalgae cultivation: A review. *Algal Research*, Elsevier. **12**, 497–512. https://doi.org/10.1016/J.ALGAL.2015.10.004

[20] Schediwy, K., Trautmann, A., Steinweg, C. and Posten, C. (2019) Microalgal kinetics — a guideline for photobioreactor design and process development. Eng Life Sci. Wiley-VCH Verlag. p. 830–43. https://doi.org/10.1002/elsc.201900107

[21] Bekirogullari, M., Figueroa-Torres, G.M., Pittman, J.K. and Theodoropoulos, C. (2020) Models of microalgal cultivation for added-value products - A review. Biotechnol Adv. Elsevier Inc. https://doi.org/10.1016/j.biotechadv.2020.107609

[22] Azmi, A.S., Aziz, N.A.C., Puad, N.I.M., Halim, A.A., Yusof, F. and Yusup, S. (2018) Chlorella vulgaris logistic growth kinetics model in high concentrations of aqueous

ammonia. *IIUM Engineering Journal*, International Islamic University Malaysia-IIUM. **19**, 1–9. https://doi.org/10.31436/iiumej.v19.i2.893

[23] Suhaida Azmi, A., Anwar Awan, M., Amid, A., Illi, N., Puad, M. and Ali, F.B. (2020) CARBON CAPTURE AND STORAGE WITH LIPID PRODUCTION IN INTEGRATED SYSTEM OF AQUEOUS AMMONIA WITH MARINE MUTANT SYNECHOCOCCUS PCC 7002 IIUM01. Biological And Natural Resources Engineering Journal.

[24] Meng, T.K. and Kassim, M.A. (2020) Growth, carbohydrate productivity and growth kinetic study of halochlorella rubescens cultivated under CO<inf>2</inf>-rich conditions. *Malaysian Applied Biology*, **49**, 1–11. https://doi.org/10.55230/mabjournal.v49i1.1647

[25] Jose, S. and Suraishkumar, G.K. (2016) High carbon (CO2) supply leads to elevated intracellular acetyl CoA levels and increased lipid accumulation in Chlorella vulgaris. *Algal Research*, Elsevier B.V. **19**, 307–15. https://doi.org/10.1016/j.algal.2016.08.011

[26] Ighalo, J.O., Dulta, K., Kurniawan, S.B., Omoarukhe, F.O., Ewuzie, U., Eshiemogie, S.O. et al. (2022) Progress in Microalgae Application for CO2 Sequestration. *Cleaner Chemical Engineering*, Elsevier. **3**, 100044. https://doi.org/10.1016/J.CLCE.2022.100044

[27] Mitra, R., Das Gupta, A., Kumar, R.R. and Sen, R. (2023) A cleaner and smarter way to achieve high microalgal biomass density coupled with facilitated self-flocculation by utilizing bicarbonate as a source of dissolved carbon dioxide. *Journal of Cleaner Production*, Elsevier. **391**, 136217. https://doi.org/10.1016/J.JCLEPRO.2023.136217

[28] Sun, Z., Bo, C., Cao, S. and Sun, L. (2025) Enhancing CO2 Fixation in Microalgal Systems: Mechanistic Insights and Bioreactor Strategies. Mar Drugs. Multidisciplinary Digital Publishing Institute (MDPI). https://doi.org/10.3390/md23030113

[29] Masojídek, J., Ranglová, K., Lakatos, G.E., Benavides, A.M.S. and Torzillo, G. (2021) Variables governing photosynthesis and growth in microalgae mass cultures. *Processes*, **9**. https://doi.org/10.3390/pr9050820

[30] Chunzhuk, E.A., Grigorenko, A. V., Kiseleva, S. V., Chernova, N.I., Vlaskin, M.S., Ryndin, K.G. et al. (2023) Effects of Light Intensity on the Growth and Biochemical Composition in Various Microalgae Grown at High CO2 Concentrations. *Plants*, Multidisciplinary Digital Publishing Institute (MDPI). **12**. https://doi.org/10.3390/plants12223876

[31] Chen, Y., Xu, C. and Vaidyanathan, S. (2020) Influence of gas management on biochemical conversion of CO<inf>2</inf> by microalgae for biofuel production. *Applied Energy*, **261**. https://doi.org/10.1016/j.apenergy.2019.114420

[32] Ashour, M., Mansour, A.T., Alkhamis, Y.A. and Elshobary, M. (2024) Usage of Chlorella and diverse microalgae for CO2 capture - towards a bioenergy revolution. *Frontiers in Bioengineering and Biotechnology*, Frontiers Media SA. **12**, 1387519. https://doi.org/10.3389/FBIOE.2024.1387519/XML

[33] Nurrusyda, F.S., Subroto, T., Hardianto, A., Sumeru, H.A., Ishmayana, S., Pratomo, U. et al. (2024) Analyzing the Impact of Physicochemical Factors on Chlorella vulgaris Growth Through Design of Experiment (DoE) for Carbon Capture System. *Molecular Biotechnology*,. https://doi.org/10.1007/s12033-023-01036-y

[34] Kumari, K., Samantaray, S., Sahoo, D. and Tripathy, B.C. (2021) Nitrogen, phosphorus and high CO2 modulate photosynthesis, biomass and lipid production in the green alga Chlorella vulgaris. *Photosynthesis Research*, Springer Science and Business Media B.V. **148**, 17–32. https://doi.org/10.1007/s11120-021-00828-0

[35] Silva, G. do N., Cerqueira, K.S., Silva, K.M., Rodrigues, J.R. da S. and Souza, R.R. de. (2023) Extraction of total carbohydrates by solvents from the microalgae Chlorella vulgaris and analysis of the influence of NaNO3 and photoperiods on

microalgae cell growth. *Brazilian Journal of Development*, South Florida Publishing LLC. **9**, 2473–87. https://doi.org/10.34117/bjdv9n1-169

[36] Valdovinos-García, E.M., Bravo-Sánchez, M.G., Olán-Acosta, M. de los Á., Barajas-Fernández, J., Guzmán-López, A. and Petriz-Prieto, M.A. (2022) Technoeconomic Evaluation of Microalgae Oil Production: Effect of Cell Disruption Method. *Fermentation*, MDPI. **8**. https://doi.org/10.3390/fermentation8070301

[37] M. Shabani and M.H. Sayadi. (2016) CO2 bio-sequestration by Chlorella vulgaris and Spirulina platensis in response to different levels of salinity and CO2. **6**, 53–61.

[38] Jeon, P.R. and Lee, C.H. (2021) Artificial neural network modelling for solubility of carbon dioxide in various aqueous solutions from pure water to brine. *Journal of CO2 Utilization*, Elsevier Ltd. **47**, 101500. https://doi.org/10.1016/j.jcou.2021.101500

[39] Aghaalipour, E., Akbulut, A. and Güllü, G. (2020) Carbon dioxide capture with microalgae species in continuous gas-supplied closed cultivation systems. *Biochemical Engineering Journal*, Elsevier. **163**, 107741. https://doi.org/10.1016/J.BEJ.2020.107741

[40] Kong, W., Shen, B., Lyu, H., Kong, J., Ma, J., Wang, Z. et al. (2021) Review on carbon dioxide fixation coupled with nutrients removal from wastewater by microalgae. *Journal of Cleaner Production*, Elsevier. **292**, 125975. https://doi.org/10.1016/J.JCLEPRO.2021.125975

[41] Hanisah, W.S., Sulaiman, W., Hanani, H., Zain, M., Othman, R., Hanie, N. et al. (2023) ALGAE CAROTENOID PIGMENTS AS NEW SOURCES OF HALAL BIOACTIVE INGREDIENTS. *Journal of Halal Science and Technology*, **2**, 68–82. https://doi.org/10.59202/jhst/v2i1.669

[42] Ayatollahi, S.Z., Esmaeilzadeh, F. and Mowla, D. (2021) Integrated CO2capture, nutrients removal and biodiesel production using Chlorella vulgaris. *Journal of Environmental Chemical Engineering*, Elsevier Ltd. **9**. https://doi.org/10.1016/j.jece.2020.104763

[43] Farahin, A.W., Natrah, I., Nagao, N., Yusoff, F.M., Shariff, M., Banerjee, S. et al. (2021) Tolerance of Tetraselmis tetrathele to High Ammonium Nitrogen and Its Effect on Growth Rate, Carotenoid, and Fatty Acids Productivity. *Frontiers in Bioengineering and Biotechnology*, Frontiers Media S.A. **9**. https://doi.org/10.3389/fbioe.2021.568776